

# Photocatalytic Hydrogen Production with A Molecular Cobalt Complex in Alkaline Aqueous Solutions

Ping Wang,<sup>†</sup> Nghia Le,<sup>‡</sup> John Daniel McCool,<sup>†</sup> Bruno Donnadieu,<sup>‡</sup> Alexander N Erickson,<sup>†</sup> Charles Edwin Webster,<sup>\*,‡</sup> Xuan Zhao<sup>\*,†</sup>

<sup>†</sup>Department of Chemistry, University of Memphis, Memphis, Tennessee 38152, United States

<sup>‡</sup>Department of Chemistry, Mississippi State University, Mississippi State, Mississippi 39762, United States

*Supporting Information Placeholder*

**ABSTRACT:** The thermodynamic favorability of alkaline solution for the oxidation of water suggests the need for developing hydrogen evolution reaction (HER) catalysts that can function in basic aqueous solutions so that both of the half reactions in overall water splitting can occur in mutually compatible solutions. Although photocatalytic HERs have been reported mostly in acidic solutions and a few at basic pHs in mixed organic aqueous solutions, visible-light driven HER catalyzed by molecular metal complexes in purely alkaline aqueous solutions remains largely unexplored. Here, we report a new cobalt complex with tetrapyridyl-amine ligand that catalyzes photolytic HER with turnover number up to 218 000 in purely aqueous solutions at pH 9.0. Density functional theory (DFT) calculation suggested a modified electron transfer (E)-proton transfer (C)-electron transfer (E)-proton transfer (C) (mod-ECEC) pathway for hydrogen production from the protonation of  $\text{Co}^{II}-\text{H}$  species. The remarkable catalytic activity resulting from subtle structural change of ligand scaffold highlights the importance of studying structure-function relationships in molecular catalyst design. Our present work significantly advances the development of molecular metal catalyst for visible-light driven HER in more challenging alkaline aqueous solutions that holds substantial promise in solar-driven water-splitting systems.

The overall splitting of water into hydrogen and oxygen, including both the oxidation of water to  $\text{O}_2$  (the oxygen evolution reaction, OER) and the reduction of protons to  $\text{H}_2$  (hydrogen evolution reaction, HER), represents a great challenge in producing clean and renewable energy sources from sunlight and/or electricity.<sup>1–3</sup> Over the past decades, significant progress has been made in developing earth-abundant metal complexes based on  $\text{Co}$ ,<sup>4–20</sup>  $\text{Ni}$ ,<sup>21–26</sup> and  $\text{Fe}$ <sup>27–31</sup> for electro- and photocatalytic hydrogen production. From the thermodynamic point of view, the OER is more favourable at basic pHs, while the HER is preferred at low pHs. Compared to HER which involves a 2-electron/2-proton process, the 4-electron/4-proton OER is energetically much more challenging. Therefore, a basic media that is preferred for OER may be more favourable for overall water splitting when occurring in the same media from the coupling of OER to HER, stressing the importance for developing HER catalysts functional at alkaline solutions.

The efficiency of electro- and photocatalytic HER is well-known to be strongly pH-dependent.<sup>32–35</sup> While electro- and/or photocatalytic hydrogen production under basic solutions have been reported for heterogeneous catalysts,<sup>36–39</sup> only a limited number of molecular metal complexes are known for HER under basic conditions.<sup>40–44</sup> The reported photocatalytic HER catalyzed by molecular catalysts under basic conditions were generally conducted in a mixture of organic solvents and aqueous solutions.<sup>40–44</sup> However, the highly oxidizing conditions needed for water oxidation suggest that organic solvents should be avoided in solar-driven water splitting devices.<sup>45</sup> To the best of our knowledge, visible-light driven HER catalyzed by molecular metal complexes in purely aqueous solutions at basic pHs has not been reported. Therefore, it remains a significant challenge in developing molecular transition metal complexes that can catalyze photolytic HER in basic aqueous solutions in the absence of any organic solvent.

We and others have reported a great number of molecular Co complexes with polypyridyl ligands for photocatalytic/electrocatalytic hydrogen production in aqueous solutions.<sup>5,13–15,46–49</sup> Our previous studies have shown that the optimal pHs for photocatalytic HER by Co complexes depend on the electronic and structural properties of ligand scaffolds.<sup>14,15</sup> While  $[\text{Co}(\text{DPA-Bpy})(\text{OH}_2)](\text{PF}_6)_3$  (**1**, DPA-Bpy = *N,N*-bis(2-pyridinylmethyl)-2,2'-bipyridine-6-methanamine, Figure 1) displays maximum HER activity at pH 4 using ascorbic acid as electron donor and  $[\text{Ru}(\text{bpy})_3]^{2+}$  as photosensitizer, the substitution of equatorial pyridyls in complex **1** with more basic isoquinoline groups shifted the optimal pH from 4 to 5 for photocatalytic HER.<sup>15</sup> The inclusion of more basic amine groups into a macrocyclic ligand of Co complex led to photocatalytic HER at an optimal pH of 6.<sup>14</sup> Furthermore, we have shown that Co complex  $[\text{Co}(\text{Py}_3\text{Me-Bpy})(\text{OH}_2)](\text{PF}_6)_2$  (**2**, Py<sub>3</sub>Me-Bpy = 6-[6-(1,1-dipyridin-2-yl-ethyl)-pyridin-2-ylmethyl]-[2,2']bipyridinyl, Figure 1) displays the highest activity for photocatalytic HER at pH 7 aqueous solutions with much improved activity and stability compared to complex **1**.<sup>48</sup> In order to further elucidate the electronic and structural factors that govern the pH-dependent photocatalytic HER, here we report the syntheses and characterizations of new Co complexes,  $[\text{Co}(\text{Py}_4\text{NMe})\text{Cl}]\text{Cl}$  (**3a**) and  $[\text{Co}(\text{Py}_4\text{NMe})(\text{OH}_2)](\text{PF}_6)_3$  (**3b**), where Py<sub>4</sub>NMe = [1-(6-(1,1-di(pyridin-2-yl)ethyl)pyridin-2-yl)-*N*-methyl-*N*-(pyridin-2-ylmethyl)methanamine] (Figure 1), which displays remarkable activity for photocatalytic HER with exceptional stability and TON of 218 000 in a pH 9 aqueous solution.

The syntheses of Py<sub>4</sub>NMe ligand and Co complexes **3a** and **3b** are shown in Scheme S1 in the Supporting Information. Alternatively, complex **3b** can be prepared from the reaction of Py<sub>4</sub>NMe ligand with [Co(CH<sub>3</sub>CN)<sub>6</sub>](PF<sub>6</sub>)<sub>2</sub> in acetone/H<sub>2</sub>O to afford complex [Co(Py<sub>4</sub>NMe)(OH<sub>2</sub>)](PF<sub>6</sub>)<sub>2</sub>·H<sub>2</sub>O (**3a'**·H<sub>2</sub>O), which can be converted to **3b** by refluxing with AgPF<sub>6</sub> in water.

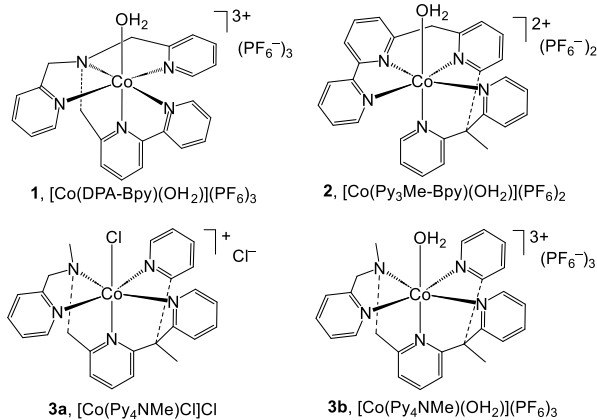


**Figure 1.** Co complexes investigated in this study.

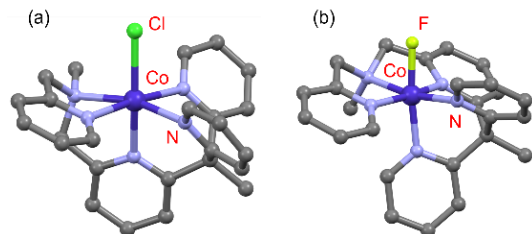


**Figure 2.** The X-ray structures of one isomer of the cations of (a) [Co(Py<sub>4</sub>NMe)Cl]Cl (**3a**) and (b) [Co(Py<sub>4</sub>NMe)(F)](PF<sub>6</sub>)<sub>2</sub>·CH<sub>3</sub>OH. Hydrogen atoms were omitted for clarity.

Figure 2a displays the crystal structure of the cation of **3a** as a distorted octahedral geometry with an axial chloride ligand. Vapor diffusion of benzene into a methanol solution of **3b** yields crystals whose X-ray structure shows the binding of a fluoride ion to the Co<sup>III</sup> center due to the decomposition of PF<sub>6</sub><sup>-</sup> anion (Figure 2b), consistent with the ESI/MS data obtained for **3b**. Furthermore, the axial chloride ligand in Figure 2a and the fluoride ligand in Figure 2b lie *trans* and *cis*, respectively, to the pyridyl linked to the -CH<sub>2</sub>N(Me)CH<sub>2</sub>Py moiety. The UV-vis spectrum of **3b** in water shows a broad peak at 488 nm from the *d-d* transition of the Co<sup>III</sup>-OH<sub>2</sub> form, similar to that of complex **1**, while no significant absorption was observed for complex **3a** in acetonitrile from 300 nm to 800 nm (Figure S3).<sup>5</sup>

The cyclic voltammogram (CV) of **3a** in CH<sub>3</sub>CN displays three quasi-reversible redox events at -0.10, -1.72, and -2.29 V (vs Fc<sup>+</sup>/Fc), corresponding to Co<sup>III</sup>/Co<sup>II</sup>, Co<sup>II</sup>/Co<sup>I</sup>, and Co<sup>I</sup>/Co<sup>0</sup> (or ligand-based) redox couples, respectively (Figure 3). The Co<sup>II</sup>/Co<sup>I</sup> couple at -1.72 V (vs Fc<sup>+</sup>/Fc) for **3** is more negative than those of the Co<sup>II</sup>-Cl forms of **1** (-1.58 V vs Fc<sup>+</sup>/Fc) and **2** (-1.54 V vs Fc<sup>+</sup>/Fc) due to the substitution of bpy group in **1** and **2** with more basic amine moiety.

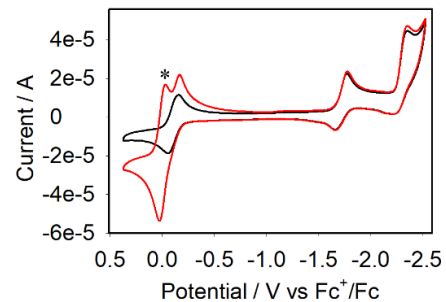


**Figure 3.** Cyclic voltammograms of **3a** (black line) and **3a** in the presence of ferrocene (red line) (redox couple for ferrocene marked with \*) in 0.1 M Bu<sub>4</sub>NPF<sub>6</sub>/CH<sub>3</sub>CN solution. Scan rate, 100 mV/s; working electrode, glassy carbon; reference electrode, Ag/AgCl; counter electrode, Pt wire; internal reference, ferrocene (\*).

In 1 M potassium phosphate solution at pH 7.0, the CV of **3a** displays a quasi-reversible redox event at 0.20 V (vs SHE) assignable to the Co<sup>III</sup>/Co<sup>II</sup> couple (Figure S4a). The Pourbaix diagram of the Co<sup>III</sup>/Co<sup>II</sup> couple of **3b** in universal buffer shows a pH dependent redox potential change from pH 3.5 to pH 11.5 with a slope of 58.5 mV/pH, suggesting a proton-coupled electron transfer (PCET) process (Figure S4b). Based on the Pourbaix diagram, the pK<sub>a</sub>'s of Co<sup>III</sup>-OH<sub>2</sub> and Co<sup>II</sup>-OH<sub>2</sub> for **3b** were derived as 3.5 and 11.5, respectively. At more negative potentials, the CV of **3b** in 1 M phosphate buffer at pH 7.0 shows one irreversible reduction event at -1.12 V (vs SHE) before catalysis (Figure 4). This event is assigned to the Co<sup>II</sup>/Co<sup>I</sup> reduction based on DFT computed value of -1.22 V (vs SHE). Compared to complexes **1** and **2**, the redox potential of -1.12 V for the Co<sup>II</sup>/Co<sup>I</sup> couple of **3b** is much more negative than those of **1** (-0.84 V) and **2** (-0.70 V vs SHE).

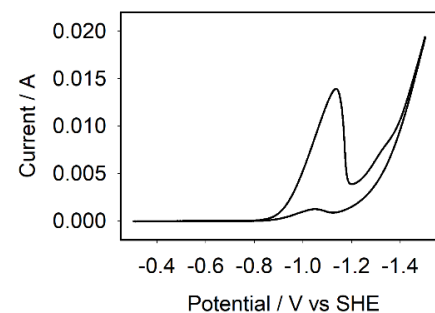


**Figure 4.** Cyclic voltammograms of **3b** (1 mM) in 1 M pH 7.0 sodium phosphate buffer. Scan rate, 100 mV s<sup>-1</sup>; working electrode, Hg pool; reference electrode, Ag/AgCl; counter electrode, Pt mesh.

Due to the higher stability of **3b** in air and its one-electron reduction leads to the formation of **3a**, only **3b** was used for the HER catalysis study. The photocatalytic HER activity of **3b** was investigated in a similar way as reported for complexes **1** and **2** using ascorbic acid as electron donor and [Ru(bpy)<sub>3</sub>]<sup>2+</sup> as photosensitizer in 0.5 M Britton-Robinson buffer.<sup>5,48</sup> At pH 7, **3b** (50 nM) catalyzed HER with a TON of 22 400, significantly higher than those previously reported for **1** and **2** at pH 7 solutions.<sup>5,48</sup> Surprisingly, a pH screening of the photocatalytic HER by **3b** demonstrated that **3b** is more active at basic aqueous solutions. At pH 9, **3b** displays the highest activity with a TON of 218 000 after ~40 h photolysis with a turnover frequency (TOF) of 12 500/h during the first 5-h photolysis (Figure 5). Under the same conditions, complexes **1**, **2** and CoSO<sub>4</sub>

produced negligible amounts of  $H_2$  close to that of control experiment in the absence of **3b** (Figure S5). Therefore, **3b** is the most active catalyst for photocatalytic HER in alkaline solutions among complexes **1-3**. Mercury poison test also confirmed the molecular nature of complex **3b** during photocatalytic HER at pH 9.0 (Figure S6). At 1.0 and 10  $\mu M$  of **3b**, the amount of  $H_2$  produced was 0.628 mmol with TON of 62 800 and 0.757 mmol with TON of 7570, respectively, demonstrating **3b** is truly effective for photocatalytic HER in basic solutions. (Figure S7).

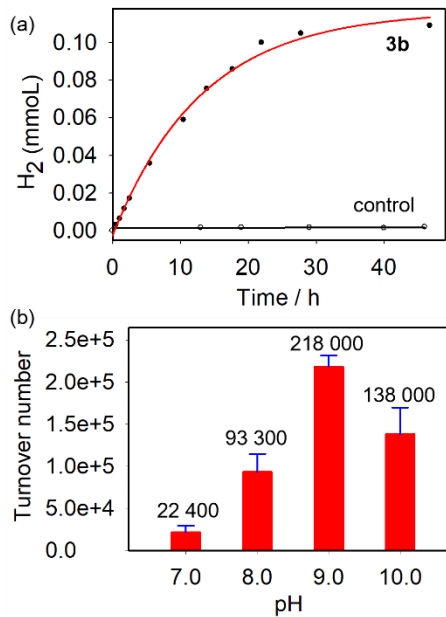


**Figure 5.** (a) Photocatalytic  $H_2$  production over time in the presence (red line) and absence (black line) of **3b**. (b) Photocatalytic  $H_2$  production at various pH values. Conditions: 10 mL of 0.5 M Britton-Robinson buffer solutions with 0.1 M ascorbic acid, 0.5 mM  $[\text{Ru}(\text{bpy})_3]^{2+}$ , and 50 nM of **3b**.

As shown in Table S2, photocatalytic HER in alkaline solutions have previously been reported for metal complexes in systems containing different photosensitizers and sacrificial electron donors at various pHs with TONs ranging from  $\sim 10$  to 11 333 in mixed organic aqueous solutions.<sup>40,41,43</sup> Our study demonstrated complex **3b** as a rare example for photocatalytic HER in alkaline aqueous solutions without using any organic solvents with a remarkable TON of 218 000 at pH 9.0. While a direct comparison of complex **3b** to the reported catalysts is unrealistic due to the different photocatalysis conditions reported in literature, the TON and TOF of **3b** are certainly among the highest reported for homogeneous photocatalytic HER in alkaline aqueous solutions.

The X-ray structures in Figure 2 demonstrate the presence of two structural isomers for the  $\text{Co}^{II}$  and  $\text{Co}^{III}$  form of **3b**. The structural isomer of the reduced  $\text{Co}^{II}$  form was considered a suitable model for DFT studies because of the reducing conditions imposed in HER catalysis, and because this structure is more favored in the formation of  $\text{Co}^{II}\text{-H}$  species. DFT computation of **3** suggests the HER catalysis can be described as a modified electron transfer (E)-proton transfer (C)-electron transfer (E)-proton transfer (C) (mod-ECEC) pathway, similar to previous studies of complexes **1** and **2**. The term 'modified' indicates an additional water dissociation step integrated with the electron and proton transfer processes. Additionally, electron and proton transfer can occur simultaneously in the form

of a proton-coupled electron transfer (PCET) step, as illustrated in Scheme S2. Our CV experiments reveal that the initial electron transfer event, which reduces  $\text{Co}^{II}$  to  $\text{Co}^{I}$  in the case of **3b**, requires more energy compared to complexes **1** and **2**. Under photolysis conditions, the reductive quenching of  $[\text{Ru}(\text{bpy})_3]^{2+}$  by ascorbate ion generates a reduced form of  $[\text{Ru}(\text{bpy})_3]^{+}$  which can reduce the Co center of complex **3b** for photocatalytic HER. While the underlying principle of photocatalysis is different from CV, it is possible to establish a correlation between the reduction events occurring at the complexes. This discrepancy in energy demands potentially gives rise to competition from the PCET step. Our computed potential of PCET energies is in general more favourable than the stepwise mechanism across all considered pH conditions (Scheme S2 and Table S3). The Gibbs reaction energy for the net reaction from  $\text{Co}^{II}\text{-H}$ , a crucial intermediate, to  $\text{Co}^{II}$  and  $H_2$  ( $\text{Co}^{II}\text{-H} + \text{H}^+ \rightarrow \text{Co}^{II} + \text{H}_2$ ) for complex **3b** was calculated to be  $-31.3$  kcal/mol (Scheme S2). Furthermore, all heterolytic coupling pathways from  $\text{Co}^{II}\text{-H}$  in Scheme S4 exhibit feasible kinetic energies.

In basic conditions with the predominance of hydroxide ions, the formation of  $\text{Co}^{II}\text{-OH}$  or  $\text{Co}^{III}\text{-OH}$  species is anticipated. The formation of hydroxo cobalt complex, in fact, does not deactivate HER catalytic activity. The  $\text{Co}^{III}\text{-OH}$  complex can undergo reduction event with a computed potential  $E(\text{Co}^{III}\text{-OH}/\text{Co}^{II}\text{-OH}) = -0.44$  V (vs SHE), followed by PCET with computed potential  $E(\text{PCET}_3) = -0.63$  V (vs SHE), leading to the production of  $\text{Co}^{I}\text{-OH}_2$  species (Scheme S2). This allows the hydroxo cobalt complexes to enter the catalytic cycle, as proposed for acidic conditions.

Previous DFT computations have suggested that the lower HER activity of complex **2** at more acidic pH conditions may result from the protonation of pyridyl groups of Py<sub>3</sub>Me-Bpy in complex **2**, resulting in the formation of an unreactive metallacycle species. The addition of tertiary amine group in complex **3** could further increase the acidic sensitivity of **3**, therefore, making it less active at lower pHs compared to higher pHs.

To gain insight into catalytic stability, we initiated an exploration of the possible decomposition pathway during catalysis. Our hypothesis is that catalyst deactivation may be linked to a pH-dependent C-C bond cleavage process, ultimately resulting in ligand breakdown. The computational results show that C-C bond cleavage transition state in basic conditions, **TS-C-C-B** is not a favourable process with  $\Delta^{\ddagger}G = 44.7$  kcal/mol. However, in acidic conditions, a protonated amine ligand can undergo the analogous process more effectively. The kinetic barrier of **TS-C-C-A** is significantly more favourable, with  $\Delta^{\ddagger}G = 22.2$  kcal/mol. Therefore, the computed energy diagram in Scheme S5 supports our hypothesis that basic conditions potentially slow down the catalyst decomposition progress of complex **3b** attributing to its higher TONs under basic solutions.

In conclusion, we have demonstrated visible light-driven hydrogen production catalyzed by a molecular Co complex in alkaline aqueous solutions that may be important for coupling to the oxidation of water for overall water splitting in alkaline solutions. Despite the subtle structural differences among complexes **1-3**, the extraordinary performance of complex **3**, in terms of both TON and TOF, for photocatalytic HER especially at basic pHs, highlight the importance of ligand design in discovering novel molecular metal complexes for future solar hydrogen production from water splitting. Further mechanistic study and ligand modifications based on complex **3b** may provide new insight into the structure-function relationships for

HER catalysis, especially in more challenging alkaline aqueous solutions.

## ASSOCIATED CONTENT

### Supporting Information

The Supporting Information is available free of charge on the ACS Publications.

Experimental details of syntheses and characterizations, and DFT computations (PDF), X-ray crystallographic data for  $[\text{Co}(\text{Py}_4\text{NMe})\text{Cl}]\text{Cl}$  (**3a**) [CCDC 2043924] and  $[\text{Co}(\text{Py}_4\text{NMe})(\text{F})](\text{PF}_6)_2 \cdot \text{CH}_3\text{OH}$  [CCDC 2295759] (CIF), Cartesian coordinates of DFT optimized structures (XYZ).

### Access Codes

CCDC 2043924 (for **3a**) and 2295759 (for  $[\text{Co}(\text{Py}_4\text{NMe})(\text{F})](\text{PF}_6)_2(\text{CH}_3\text{OH})$ ) contain the supplementary crystallographic data for this paper. These data can be obtained free of charge via [www.ccdc.cam.ac.uk/data\\_request/cif](http://www.ccdc.cam.ac.uk/data_request/cif), or by emailing [data\\_request@ccdc.cam.ac.uk](mailto:data_request@ccdc.cam.ac.uk), or by contacting The Cambridge Crystallographic Data Centre, 12 Union Road, Cambridge CB2 1EZ, U.K.; fax: +44 1223 336033.

## AUTHOR INFORMATION

### Corresponding Author

\*[ewebster@chemistry.msstate.edu](mailto:ewebster@chemistry.msstate.edu)

\*[xzhao1@memphis.edu](mailto:xzhao1@memphis.edu)

### ORCID

Ping Wang: 0000-0002-5015-0985

Nghia Le: 0000-0003-2472-0806

John Daniel McCool: 0009-0004-2652-5195

Bruno Donnadieu: 0000-0002-0655-0578

Alexander N Erickson: 0009-0007-5837-0978

Charles Edwin Webster: 0000-0002-6917-2957

Xuan Zhao: 0000-0003-3019-2261

### Notes

The authors declare no competing financial interests.

## ACKNOWLEDGMENT

This work is supported by National Science Foundation, CAREER CHE-1352036, CHE-2018806 and CHE-2102265 to X.Z., CHE-1800201 and CHE-2102552 to C.E.W. We thank the Department of Chemistry at The University of Memphis and the Department of Chemistry at Mississippi State University. The computational work was supported by the Mississippi State University High Performance Computing Collaboratory (HPC) and the Mississippi Center for Supercomputing Research (MCSR).

## REFERENCES

- (1) Lewis, N. S.; Nocera, D. G. Powering the Planet: Chemical Challenges in Solar Energy Utilization. *Proc. Natl. Acad. Sci. U. S. A.* **2006**, *103*, 15729-15735.
- (2) Gray, H. B. Powering the planet with solar fuel. *Nat. Chem.* **2009**, *1*, 7-7.
- (3) Youngblood, W. J.; Lee, S.-H. A.; Maeda, K.; Mallouk, T. E. Visible Light Water Splitting using Dye-Sensitized Oxide Semiconductors. *Acc. Chem. Res.* **2009**, *42*, 1966-1973.
- (4) Sun, Y.; Bigi, J. P.; Piro, N. A.; Tang, M. L.; Long, J. R.; Chang, C. J. Molecular Cobalt Pentapyridine Catalysts for Generating Hydrogen from Water. *J. Am. Chem. Soc.* **2011**, *133*, 9212-9215.
- (5) Singh, W. M.; Baine, T.; Kudo, S.; Tian, S.; Ma, X. A. N.; Zhou, H.; DeYonker, N. J.; Pham, T. C.; Bollinger, J. C.; Baker, D. L.; Yan, B.; Webster, C. E.; Zhao, X. Electrocatalytic and Photocatalytic Hydrogen Production in Aqueous Solution by a Molecular Cobalt Complex. *Angew. Chem., Int. Ed.* **2012**, *51*, 5941-5944.
- (6) Bachmann, C.; Guttentag, M.; Spangler, B.; Alberto, R. 3d Element Complexes of Pentadentate Bipyridine-Pyridine-Based Ligand Scaffolds: Structures and Photocatalytic Activities. *Inorg. Chem.* **2013**, *52*, 6055-6061.
- (7) Zhang, P.; Wang, M.; Gloaguen, F.; Chen, L.; Quentel, F.; Sun, L. Electrocatalytic hydrogen evolution from neutral water by molecular cobalt tripyridine-diamine complexes. *Chem. Commun.* **2013**, *49*, 9455-9457.
- (8) Call, A.; Codolà, Z.; Acuña-Parés, F.; Lloret-Fillol, J. Photo- and Electrocatalytic H<sub>2</sub> Production by New First-Row Transition-Metal Complexes Based on an Aminopyridine Pentadentate Ligand. *Chem. Euro. J.* **2014**, *20*, 6171-6183.
- (9) Kawano, K.; Yamauchi, K.; Sakai, K. A cobalt-NHC complex as an improved catalyst for photochemical hydrogen evolution from water. *Chem. Commun.* **2014**, *50*, 9872-9875.
- (10) Tong, L.; Zong, R.; Thummel, R. P. Visible Light-Driven Hydrogen Evolution from Water Catalyzed by A Molecular Cobalt Complex. *J. Am. Chem. Soc.* **2014**, *136*, 4881-4884.
- (11) Basu, D.; Mazumder, S.; Shi, X.; Baydoun, H.; Niklas, J.; Poluektov, O.; Schlegel, H. B.; Verani, C. N. Ligand Transformations and Efficient Proton/Water Reduction with Cobalt Catalysts Based on Pentadentate Pyridine-Rich Environments. *Angew. Chem., Int. Ed.* **2015**, *54*, 2105-2110.
- (12) Firpo, V.; Le, J. M.; Pavone, V.; Lombardi, A.; Bren, K. L. Hydrogen evolution from water catalyzed by cobalt-mimochrome VI\*<sup>a</sup>, a synthetic mini-protein. *Chem. Sci.* **2018**, *9*, 8582-8589.
- (13) Wang, P.; Liang, G.; Reddy, M. R.; Long, M.; Driskill, K.; Lyons, C.; Donnadieu, B.; Bollinger, J. C.; Webster, C. E.; Zhao, X. Electronic and Steric Tuning of Catalytic H<sub>2</sub> Evolution by Cobalt Complexes with Pentadentate Polypyridyl-Amine Ligands. *J. Am. Chem. Soc.* **2018**, *140*, 9219-9229.
- (14) Wang, P.; Liang, G.; Boyd, C. L.; Webster, C. E.; Zhao, X. Catalytic H<sub>2</sub> Evolution by a Mononuclear Cobalt Complex with a Macroyclic Pentadentate Ligand. *Eur. J. Inorg. Chem.* **2019**, *2134-2139*.
- (15) Vennampalli, M.; Liang, G.; Katta, L.; Webster, C. E.; Zhao, X. Electronic Effects on a Mononuclear Co Complex with a Pentadentate Ligand for Catalytic H<sub>2</sub> Evolution. *Inorg. Chem.* **2014**, *53*, 10094-10100.
- (16) Queyriaux, N.; Sun, D.; Fize, J.; Pecaut, J.; Field, M. J.; Chavaroche-Kerlidou, M.; Artero, V. Electrocatalytic Hydrogen Evolution with a Cobalt Complex Bearing Pendant Proton Relays: Acid Strength and Applied Potential Govern Mechanism and Stability. *J. Am. Chem. Soc.* **2020**, *142*, 274-282.
- (17) Alvarez-Hernandez, J. L.; Sopchak, A. E.; Bren, K. L. Buffer pKa Impacts the Mechanism of Hydrogen Evolution Catalyzed by a Cobalt Porphyrin-Peptide. *Inorg. Chem.* **2020**, *59*, 8061-8069.
- (18) Kohler, L.; Niklas, J.; Johnson, R. C.; Zeller, M.; Poluektov, O. G.; Mulfort, K. L. Molecular Cobalt Catalysts for H<sub>2</sub> Generation with Redox Activity and Proton Relays in the Second Coordination Sphere. *Inorg. Chem.* **2019**, *58*, 1697-1709.
- (19) Chen, L.; Khadivi, A.; Singh, M.; Jurss, J. W. Synthesis of a pentadentate, polypyrazine ligand and its application in cobalt-catalyzed hydrogen production. *Inorg. Chem. Front.* **2017**, *4*, 1649-1653.
- (20) Jurss, J. W.; Khnayzer, R. S.; Panetier, J. A.; El Roz, K. A.; Nichols, E. M.; Head-Gordon, M.; Long, J. R.; Castellano, F. N.; Chang, C. J. Bioinspired design of redox-active ligands for multielectron catalysis: effects of positioning pyrazine reservoirs on cobalt for electro- and photocatalytic generation of hydrogen from water. *Chem. Sci.* **2015**, *6*, 4954-4972.
- (21) Helm, M. L.; Stewart, M. P.; Bullock, R. M.; DuBois, M. R.; DuBois, D. L. A synthetic nickel electrocatalyst with a turnover

frequency above 100,000 s(-)(1) for H<sub>2</sub> production. *Science* **2011**, *333*, 863-866.

(22) Han, Z.; Shen, L.; Brennessel, W. W.; Holland, P. L.; Eisenberg, R. Nickel pyridinethiolate complexes as catalysts for the light-driven production of hydrogen from aqueous solutions in noble-metal-free systems. *J. Am. Chem. Soc.* **2013**, *135*, 14659-14669.

(23) Gan, L.; Groy, T. L.; Tarakeshwar, P.; Mazinani, S. K.; Shearer, J.; Mujica, V.; Jones, A. K. A nickel phosphine complex as a fast and efficient hydrogen production catalyst. *J Am Chem Soc* **2015**, *137*, 1109-1115.

(24) Tatematsu, R.; Inomata, T.; Ozawa, T.; Masuda, H. Electrocatalytic Hydrogen Production by a Nickel(II) Complex with a Phosphinopyridyl Ligand. *Angew. Chem., Int. Ed.* **2016**, *55*, 5247-5250.

(25) Zhao, X.; Feng, J.; Liu, J.; Shi, W.; Yang, G.; Wang, G.-C.; Cheng, P. An Efficient, Visible-Light-Driven, Hydrogen Evolution Catalyst NiS/ZnxCd1-xS Nanocrystal Derived from a Metal-Organic Framework. *Angew. Chem., Int. Ed.* **2018**, *57*, 9790-9794.

(26) Yang, J. Y.; Bullock, R. M.; DuBois, M. R.; DuBois, D. L. Fast and efficient molecular electrocatalysts for H<sub>2</sub> production: using hydrogenase enzymes as guides. *MRS Bull.* **2011**, *36*, 39-47.

(27) Schilter, D.; Camara, J. M.; Huynh, M. T.; Hammes-Schiffer, S.; Rauchfuss, T. B. Hydrogenase Enzymes and Their Synthetic Models: The Role of Metal Hydrides. *Chem. Rev.* **2016**, *116*, 8693-8749.

(28) Wang, F.; Wang, W.-G.; Wang, X.-J.; Wang, H.-Y.; Tung, C.-H.; Wu, L.-Z. A Highly Efficient Photocatalytic System for Hydrogen Production by a Robust Hydrogenase Mimic in an Aqueous Solution. *Angew. Chem., Int. Ed.* **2011**, *50*, 3193-3197.

(29) Rose, M. J.; Gray, H. B.; Winkler, J. R. Hydrogen Generation Catalyzed by Fluorinated Diglyoxime-Iron Complexes at Low Overpotentials. *J. Am. Chem. Soc.* **2012**, *134*, 8310-8313.

(30) Kaur-Ghumaan, S.; Schwartz, L.; Lomoth, R.; Stein, M.; Ott, S. Catalytic Hydrogen Evolution from Mononuclear Iron(II) Carbonyl Complexes as Minimal Functional Models of the [FeFe] Hydrogenase Active Site. *Angew. Chem., Int. Ed.* **2010**, *49*, 8033-8036.

(31) Ding, S.; Ghosh, P.; Lunsford, A. M.; Wang, N.; Bhuvanesh, N.; Hall, M. B.; Darensbourg, M. Y. Hemilabile Bridging Thiolates as Proton Shuttles in Bioinspired H<sub>2</sub> Production Electrocatalysts. *J. Am. Chem. Soc.* **2016**, *138*, 12920-12927.

(32) Reynal, A.; Pastor, E.; Gross, M. A.; Selim, S.; Reisner, E.; Durrant, J. R. Unravelling the pH-dependence of a molecular photocatalytic system for hydrogen production. *Chem. Sci.* **2015**, *6*, 4855-4859.

(33) Horvath, S.; Fernandez, L. E.; Appel, A. M.; Hammes-Schiffer, S. pH-Dependent Reduction Potentials and Proton-Coupled Electron Transfer Mechanisms in Hydrogen-Producing Nickel Molecular Electrocatalysts. *Inorg. Chem.* **2013**, *52*, 3643-3652.

(34) Fukuzumi, S.; Kobayashi, T.; Suenobu, T. Photocatalytic Production of Hydrogen by Disproportionation of One-Electron-Reduced Rhodium and Iridium-Ruthenium Complexes in Water. *Angew. Chem., Int. Ed.* **2011**, *50*, 728-731.

(35) Appel, A. M.; Pool, D. H.; O'Hagan, M.; Shaw, W. J.; Yang, J. Y.; Rakowski DuBois, M.; DuBois, D. L.; Bullock, R. M. [Ni(PPh<sub>2</sub>NBn<sub>2</sub>)<sub>2</sub>(CH<sub>3</sub>CN)]<sup>2+</sup> as an Electrocatalyst for H<sub>2</sub> Production: Dependence on Acid Strength and Isomer Distribution. *ACS Catal.* **2011**, *1*, 777-785.

(36) Wang, C.; Cao, S.; Fu, W.-F. A stable dual-functional system of visible-light-driven Ni(II) reduction to a nickel nanoparticle catalyst and robust *in situ* hydrogen production. *Chem. Commun.* **2013**, *49*, 11251-11253.

(37) Li, W.; Liu, Y.; Wu, M.; Feng, X.; Redfern, S. A. T.; Shang, Y.; Yong, X.; Feng, T.; Wu, K.; Liu, Z.; Li, B.; Chen, Z.; Tse, J. S.; Lu, S.; Yang, B. Carbon-Quantum-Dots-Loaded Ruthenium Nanoparticles as an Efficient Electrocatalyst for Hydrogen Production in Alkaline Media. *Adv. Mater.* **2018**, *30*, 1800676.

(38) Vrubel, H.; Hu, X. Molybdenum Boride and Carbide Catalyze Hydrogen Evolution in both Acidic and Basic Solutions. *Angew. Chem., Int. Ed.* **2012**, *51*, 12703-12706.

(39) Song, F.; Li, W.; Yang, J.; Han, G.; Liao, P.; Sun, Y. Interfacing nickel nitride and nickel boosts both electrocatalytic hydrogen evolution and oxidation reactions. *Nat. Commun.* **2018**, *9*, 4531.

(40) Song, X.; Wen, H.; Ma, C.; Chen, H.; Chen, C. Hydrogen photogeneration catalyzed by a cobalt complex of a pentadentate aminopyridine-based ligand. *New J. Chem.* **2015**, *39*, 1734-1741.

(41) Du, P.; Knowles, K.; Eisenberg, R. A Homogeneous System for the Photogeneration of Hydrogen from Water Based on a Platinum(II) Terpyridyl Acetylide Chromophore and a Molecular Cobalt Catalyst. *J. Am. Chem. Soc.* **2008**, *130*, 12576-12577.

(42) Zhang, P.; Wang, M.; Na, Y.; Li, X.; Jiang, Y.; Sun, L. Homogeneous photocatalytic production of hydrogen from water by a bioinspired [Fe<sub>2</sub>S<sub>2</sub>] catalyst with high turnover numbers. *Dalton Trans.* **2010**, *39*, 1204-1206.

(43) Panagiotakis, S.; Landrou, G.; Nikolaou, V.; Putri, A.; Hardré, R.; Massin, J.; Charalambidis, G.; Coutsolelos, A. G.; Orio, M. Efficient Light-Driven Hydrogen Evolution Using a Thiosemicarbazone-Nickel (II) Complex. *Front Chem* **2019**, *7*, 405-405.

(44) Li, C.-B.; Chu, Y.; He, J.; Xie, J.; Liu, J.; Wang, N.; Tang, J. Photocatalytic Hydrogen Production Based on a Serial Metal-Salen Complexes and the Reaction Mechanism. *ChemCatChem* **2019**, *11*, 6324-6331.

(45) McKone, J. R.; Lewis, N. S.; Gray, H. B. Will Solar-Driven Water-Splitting Devices See the Light of Day? *Chem. Mater.* **2014**, *26*, 407-414.

(46) Shan, B.; Baine, T.; Ma, X. A. N.; Zhao, X.; Schmehl, R. H. Mechanistic Details for Cobalt Catalyzed Photochemical Hydrogen Production in Aqueous Solution: Efficiencies of the Photochemical and Non-Photochemical Steps. *Inorg. Chem.* **2013**, *52*, 4853-4859.

(47) Lewandowska-Andralojc, A.; Baine, T.; Zhao, X.; Muckerman, J. T.; Fujita, E.; Polyansky, D. E. Mechanistic studies of hydrogen evolution in aqueous solution catalyzed by a terpyridine-amine cobalt complex. *Inorg. Chem.* **2015**, *54*, 4310-4321.

(48) Wang, P.; Liang, G.; Smith, N.; Hill, K.; Donnadieu, B.; Webster, C. E.; Zhao, X. Enhanced Hydrogen Evolution in Neutral Water Catalyzed by a Cobalt Complex with a Softer Polypyridyl Ligand. *Angew. Chem., Int. Ed.* **2020**, *59*, 12694-12697.

(49) Wang, P.; Liang, G.; Webster, C. E.; Zhao, X. Structure-Functional Analysis of Hydrogen Production Catalyzed by Molecular Cobalt Complexes with Pentadentate Ligands in Aqueous Solutions. *Eur. J. Inorg. Chem.* **2020**, 3534-3547.

## Table of Contents Graphic

